Journal of Nano- and Electronic Physics
Vol. **14** No 3, 03015(5pp) (2022)

Журнал нано- та електронної фізики
Том **14** № 3, 03015(5cc) (2022)

Numerical Analysis of Performance of Various ETL Materials for Cesium Titanium (IV) Single Halide Based PSCs

Kunal Chakraborty[1], S.V. Kumari[2], Sri Harsha Arigela[3], Mahua Gupta Choudhury[1], Sudipta Das[4], Samrat Paul[1,*]

[1] *Department of Energy Engineering, North-Eastern Hill University, Shillong, Meghalaya, India*
[2] *Department of ECE, NRI Institute of Technology, Agiripalli, Krishna Dist, AP, India*
[3] *Department of Mechanical Engineering, Koneru Lakshmaiah Education Foundation, Guntur, AP, India*
[4] *Department of ECE, IMPS College of Engineering and Technology, Nityanandapur, Malda, W.B, India*

(Received 24 March 2022; revised manuscript received 25 June 2022; published online 30 June 2022)

Lead-free perovskite solar cells (PSCs) appear to be a great contender of thin film based photovoltaic (PV) technology as they solve two prime issues, toxicity and stability. Ti-based PSCs can be imperative in a high-performance PV device. The external quantum efficiency (EQE) or classical efficiency is often used to measure the optical performance of the solar cell device. This work has a scope in optimizing ETL/HTL and other interfaces to obtain the most efficient $Cs_2TiI_{6-x}Br_x$ PSC, and enhancement in J_{sc} will increase the Shockley-Read-Hall (SRH) recombination. In such circumstances, selection and optimization of electron transport layers (ETLs) and hole transport layers (HTLs) materials are the major factor to be considered effectively to achieve optimum PV performance. Among all ETLs, TiO_2 is found to be the most suitable ETL for our proposed FTO/ETLs/Cs_2TiX_6/HTL/Ag based *n*-i-*p* structured PSCs. The optimum thickness of ETL should be 150-200 nm and of HTL – 10-20 nm, with the following optimized PV performance: V_{oc} = 1.23 V, J_{sc} = 19.378 mA/cm², PCE = 14.537 % (Cs_2TiBr_6); V_{oc} = 1.09 V, J_{sc} = 23.213 mA/cm², PCE = 17.452 % (Cs_2TiI_6); V_{oc} = 1.53 V, J_{sc} = 16.822 mA/cm², PCE = 12.578 % (Cs_2TiF_6) and V_{oc} = 8.53 V, J_{sc} = 10.079 mA/cm², PCE = 7.348 % (Cs_2TiCl_6). Thus, a detailed study of this class of materials containing halide perovskite is need of the hour.

Keywords: Halide, Perovskite, SCAPS-1D, Photovoltaic, PCE.

DOI: 10.21272/jnep.14(3).03015 PACS number: 88.40.hj

1. INTRODUCTION

Global GDP is increasing at 3.25 % per year and the global population will reach to 9.2 billion by 2040. Higher living standard causes increase in energy demand. Economies of the developing nation's account for above 80 % expansion in world's output. As with GDP growth, the vast majority of this increase stems from increasing prosperity, people move from low to middle income group, allowing them to increase substantially their per capita energy consumption. The overall growth in energy demand is materially offset by declines in energy intensity (energy used per unit of GDP). Third-generation thin film based solar cell like Perovskite solar cell (PSC) has great potential in the Photovoltaic (PV) technology due to its simple fabrication process and lower manufacturing cost [1]. But for the commercialization of PSC, it must meet certain aspects related to the challenges and standards which are mainly stability, hysteresis, and device structure during the manufacturing of the device. A typical PSC employed organic-inorganic hybrid halide material ($MAPbX_3$ and $FAPbX_3$) as active material [2-4]. The power conversion efficiency (PCE) of such device has increased from 3.8 % in 2009 to 25 % in 2020 [5, 6]. Despite of having such advantages, organic-inorganic hybrid active material has three major concerns such as lower shelf life, stability and toxicity. These issues can be overcome through the Pb-free PSCs [7-11]. Ahmed et al. made a theoretical predication using TiO_2/Cs_2TiBr_6 structure PSC and achieved 11.9 % PCE [12]. Ju et al. made both experimental as well as theoretical study on earth abundant Ti-based Cs_2TiX_6 based PSC with the 1.0 to 1.8 eV tunable band gap exhibits double Perovskite structure [13]. Chen et al. with his experimental study showed Cs_2TiBr_6 PSC has great potential of PV performance with 1.8 eV band gap [14]. Nitin et al. showed a numerical simulation study about impact of various electron transport layers (ETLs), hole transport layers (HTLs) materials on the PV performance of the device [15].

In this work, we have proposed a FTO/ETLs/Cs_2TiX_6 (X = Br, I, F and Cl)/HTL/Ag based *n*-i-*p* PSC structure to select a suitable pair of ETL/absorber and absorber/HTL which has higher photovoltaic performance, followed by optimization of ETL, HTL material using the SCAPS 1D-3.3.2.0 simulator.

2. SIMULATION

The proposed 1D *n*-i-*p* planar device structure comprises FTO/ETLs/Cs_2TiX_6/HTL/Ag has been studied under the ambient condition using the SCAPS simulator and which was illustrated in the Fig. 1a. In this heterojunction structure we have used five different n-region ETLs *n*-WO_3, *n*-TiO2, *n*-SnO_2, *n*-ZnO, *n*-CdS; four different i-region absorbing layer i-Cs_2TiBr_6, i-Cs_2TiI_6, i-Cs_2TiF_6, i-Cs_2TiCl_6; and one *p*-region *p*-HTL material CuSCN. To validate our simulation result with the experimental result we have taken the various device parameters value from the literature [16-20]. The details of the various parameters viz. thickness, E_g

* paulsamrat17 @gmail.com
The results were presented at the 2nd International Conference on Innovative Research in Renewable Energy Technologies (IRRET-2022)

(band gap), E_a (electron affinity), ε_r (relative permittivity), N_D (donor density), N_A (acceptor density), μ_n (electron mobility) and μ_p (hole mobility) are described in the literature review [10-15]. The work function of FTO and Ag is lies between 4.26-4.74 eV, type of defect is neutral with the energetic Gaussian distribution where characteristic energy level is 0.1 eV with respect to reference level of 0.6 eV. The thermal velocity of both electrons and holes are 107 cm/s at the operating temperature 300 K [16-18]. The energy level diagram of the different ETLs and HTL material has been shown in Fig. 1b.

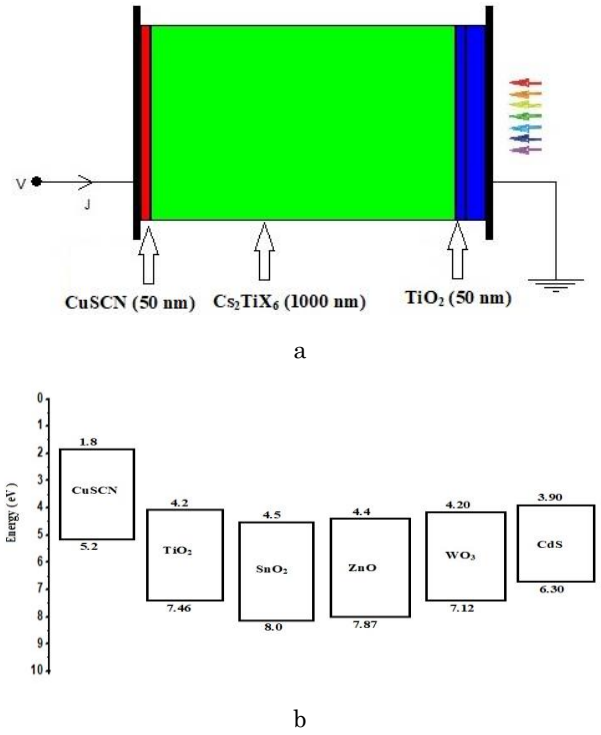

Fig. 1 – Schematic diagram of FTO/ETLs/Cs_2TiX_6/HTL/Ag based PSC in the SCAPS simulator (a) Schematic band diagram of the different ETLs and HTL material (b)

3. RESULTS AND DISCUSSION

In this section, the performance of the device has been analyzed with the different ETL materials (TiO_2, SnO_2, ZnO, WO_3 and CdS), HTL material (CuSCN) and then optimize the thickness of the ETL, HTL.

3.1 Performance of the Device with Different ETL Materials

The *J-V* curve of the device for the different ETL materials was estimated by the SCAPS-1D simulation with the data given in Tables 1, 2 and 3. Fig. 2a, 2b, 2c and 2d, indicating the *J-V* curve of the Cs_2TiBr_6, Cs_2TiI_6, Cs_2TiF_6 and Cs_2TiCl_6 absorbing layer with different ETL materials, and it shows TiO_2, SnO_2 and WO_3 has better photovoltaic performance in terms of transmittance and current conductivity [16]. The V_{OC} and J_{SC} value with the TiO_2 ETL for the Cs_2TiBr_6, Cs_2TiI_6, Cs_2TiF_6 and Cs_2TiCl_6 absorbing layer was estimated as 1.23 V, 1.09 V, 1.53 V, 8.53 V and 19.4 mA/cm^2, 23.2 mA/cm^2, 16.8 mA/cm^2, 8.53 mA/cm^2 which is better than that of SnO_2 and WO_3 ETL. The V_{OC} for the SnO_2 and WO_3 ETL is 1.23 V, 1.09 V, 1.53 V, 8.51 V and 1.21 V, 1.08 V, 1.46 V, 8.45 V respectively for the Cs_2TiBr_6, Cs_2TiI_6, Cs_2TiF_6 and Cs_2TiCl_6 absorbing layer based device. The QE of the Cs_2TiBr_6, Cs_2TiI_6, Cs_2TiF_6 and Cs_2TiCl_6 absorbing layer based Perovskite solar cell (PSC) is defined in Fig. 3a, 3b, 3c and 3d for the different ETL materials under the 100-800 nm wavelength. From the QE plot shown in Fig. 3a, it is clearly visible that by increasing the wavelength of 100-370 nm the QE increases and after that QE is constant up to 580 nm followed by it is started to decrease gradually up to 700 nm for the Cs_2TiBr_6 absorbing layer based solar cell device. On the other side, Fig. 3b, Fig. 3c and Fig. 3d show that QE plot increases up to 380 nm wavelength for the Cs_2TiI_6, Cs_2TiF_6 and Cs_2TiCl_6 absorbing layer based device. This value indicates that the production of current by the PSC is higher due to the irradiation of photons [12]. By analyzing the photovoltaic (PV)

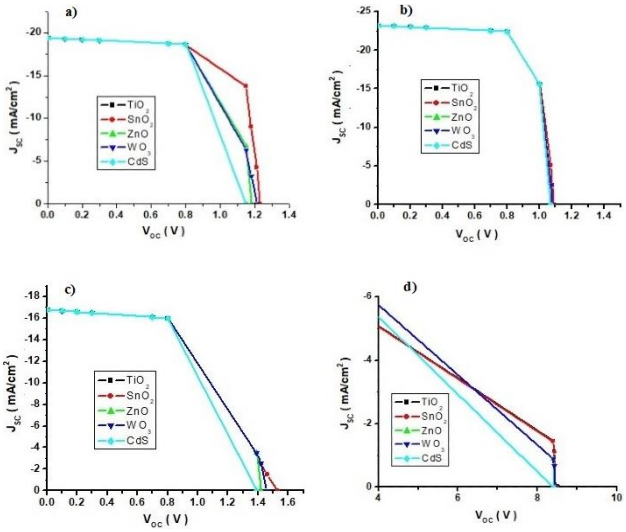

Fig. 2 – *J-V* graph for: (a) Cs_2TiBr_6, (b) Cs_2TiI_6, (c) Cs_2TiF_6 and (d) Cs_2TiCl_6 absorbing layer based PSCs

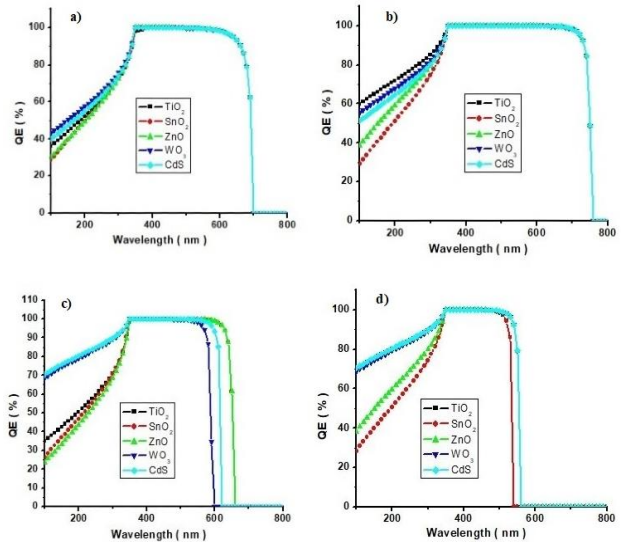

Fig. 3 – QE plot for: (a) Cs_2TiBr_6, (b) Cs_2TiI_6, (c) Cs_2TiF_6 and (d) Cs_2TiCl_6 absorbing layer based PSCs

performance of the ETLs in the Cs_2TiBr_6, Cs_2TiI_6, Cs_2TiF_6 and Cs_2TiCl_6 absorbing layer based device, we found that TiO_2 would be the suitable ETL material to achieve the optimum photovoltaic performance of the device.

Cs_2TiF_6 active layer based PSC where the PV performance of the PSCs as follows: V_{OC} = 1.2297 V, PCE = 14.532 % (Cs_2TiBr_6 PSC); V_{OC} = 1.0899 V, PCE = 17.452 % (Cs_2TiI_6 PSC), V_{OC} = 1.5294 V, PCE = 12.573 % (Cs_2TiF_6 PSC) and 20 nm for Cs_2TiCl_6 absorbing.

3.2 Optimization of ETL Material

The thickness optimization of TiO_2 ETL material is plays an important role to reach the optimum PV performance of the PSC [10]. Here, Fig. 4a, 4b, 4c and 4d indicating the V_{OC}, PCE curve with the variation of ETL layer thickness for the Cs_2TiBr_6, Cs_2TiI_6, Cs_2TiF_6 and Cs_2TiCl_6 absorbing layer device. From Fig. 4a, 4b, 4c it is clearly observed that V_{OC} decreases continuously as the thickness of TiO_2 ETL increases. On the other hand, initially PCE increases up to 400 nm thickness for Cs_2TiBr_6 PSC, up to 180 nm thickness for Cs_2TiI_6, Cs_2TiF_6 PSC. The reason behind this deterioration in the V_{OC}, PCE is the rises of electron-hole pair recombination as a result series resistance increases which will form uneven surface and pinholes. Similarly, by looking at Fig. 4d, both V_{OC} and PCE increase with the ETL thickness for the Cs_2TiCl_6 PSC. The prime reason behind this increase in V_{OC} and PCE is lowering of device series resistance which leads to increases in the conductivity of the active material. Such phenomenon will enhance the carrier concentration and carrier mobility. So, by considering all the PV performance the optimum thickness of the TiO_2 ETL would be 150 nm for the Cs_2TiBr_6, Cs_2TiI_6, Cs_2TiF_6 absorbing layer PSC and 200 nm for the Cs_2TiCl_6 absorbing layer PSC.

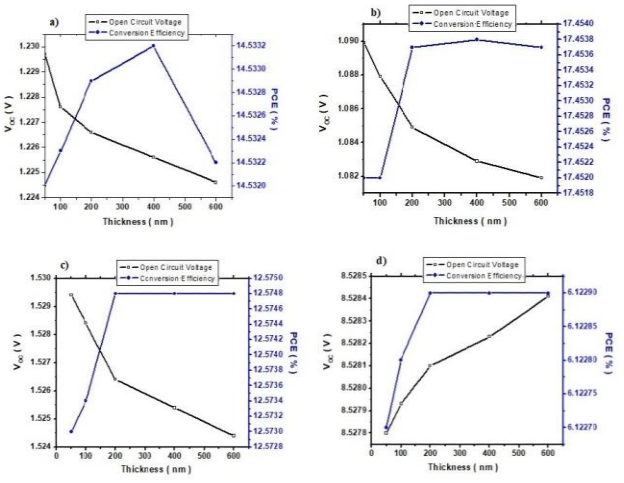

Fig. 4 – PV performance of the: (a) Cs_2TiBr_6, (b) Cs_2TiI_6, (c) Cs_2TiF_6 and (d) Cs_2TiCl_6 absorbing layer based PSCs with ETL thickness variation

3.3 Optimization of HTL Material

In this section, we analyze the effect of CuSCN HTL material in PSC and optimum thickness value of the HTL. Here, Fig. 5a, 5b, 5c and 5d, indicating the V_{OC} and PCE variation of the Cs_2TiBr_6, Cs_2TiI_6, Cs_2TiF_6 and Cs_2TiCl_6 PSC with the HTL thickness. It was observed that V_{OC} decreases abruptly along with the slight fall in the PCE for the Cs_2TiBr_6, Cs_2TiI_6, Cs_2TiF_6 PSC. This incident attributed to the device junction resistance. Thus, lower amount of charge was collected at the HTL/absorber interface with Cs_2TiBr_6, Cs_2TiI_6, Cs_2TiF_6 PSC as the thickness of the ETL increases. On the other side, for the Cs_2TiCl_6 PSC, V_{OC} decreases up to 40 nm HTL thickness and after that V_{OC} remained constant whereas, PCE increases up to 100 nm and after that it become constant which indicates higher collection of charge at the HTL/absorber interface. Hence, the optimized HTL (CuSCN) thickness was found to be 10 nm for the Cs_2TiBr_6, Cs_2TiI_6, layer PSC where PV performance was recorded as: V_{OC} = 8.5278 V, PCE = 6.1227 %.

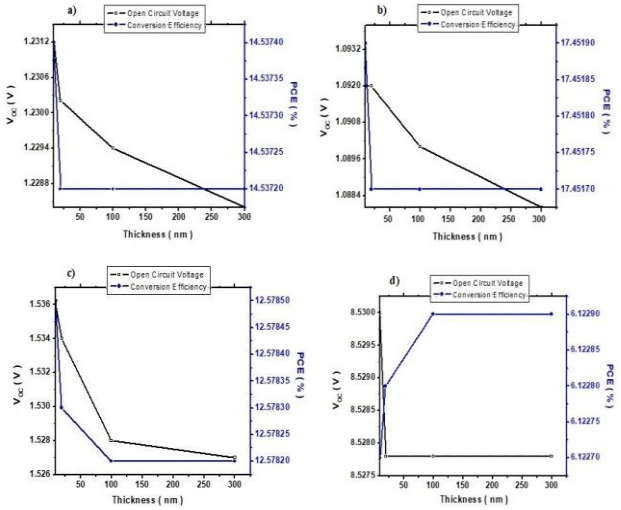

Fig. 5 – PV performance of the: (a) Cs_2TiBr_6, (b) Cs_2TiI_6, (c) Cs_2TiF_6 and (d) Cs_2TiCl_6 absorbing layer based PSC with HTL thickness variation

3.4 Optimized Device Model

In this section, we have proposed the device model by considering the optimized values of the ETL, HTL layer thickness which is shown at Fig. 6. The optimized PV parameters are obtained as follows: V_{OC} = 1.23 V, J_{SC} = 19.378 mA/cm^2, PCE = 14.537% (Cs_2TiBr_6 PSC); V_{OC} = 1.09 V, J_{SC} = 23.213 mA/cm^2, PCE = 17.452% (Cs_2TiI_6 PSC); V_{OC} = 1.53 V, J_{SC} = 16.822 mA/cm^2, PCE = 12.578% (Cs_2TiF_6 PSC) and V_{OC} = 8.53 V, J_{SC} = 10.079 mA/cm^2, PCE = 7.348 % (Cs_2TiCl_6 PSC). The optimized QE of the Cs_2TiBr_6, Cs_2TiI_6, Cs_2TiF_6 and Cs_2TiCl_6 absorbing material based PSC is shown in the Fig. 7. From this it is clearly observed that Cs_2TiBr_6, Cs_2TiI_6, Cs_2TiF_6 and Cs_2TiCl_6 absorbing material is visible up to 700 nm, 760 nm, 680 nm and 580 nm wavelength approximately. The variation of the simulated and experimental result indicates the process of optimization of the materials and device has been carried out under the ideal condition as a result degradation and surface morphology process has been ignored.

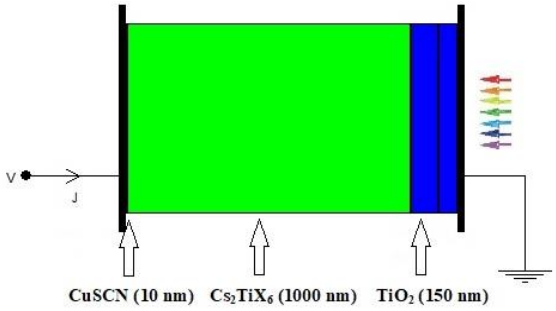

Fig. 6 – Schematic diagram of optimized FTO/ETLs/Cs_2TiX_6/HTL/Ag based PSC device

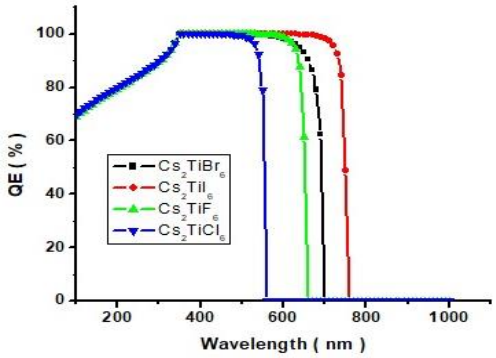

Fig. 7 – Optimized QE plot for: (a) Cs_2TiBr_6, (b) Cs_2TiI_6, (c) Cs_2TiF_6 and (d) Cs_2TiCl_6 absorbing layer based PSCs

4. CONCLUSIONS

In this present work, we have simulated the Cs_2TiBr_6, Cs_2TiI_6, Cs_2TiF_6 and Cs_2TiCl_6 absorbing material PSC using the different inorganic ETLs. Here, TiO_2 was found most suitable ETL among all other ETLs and the optimized thickness of TiO_2 ETL was 150-200 nm whereas the HTL (CuSCN) layer was optimized at 10-20 nm for the Cs_2TiX_6 (X = Br, I, F and Cl) PSC. The proposed PSC device shows an excellent PV performance at the optimized condition as V_{OC} = 1.23 V, PCE = 14.537 % (Cs_2TiBr_6); V_{OC} = 1.09 V, PCE = 17.452 % (Cs_2TiI_6); V_{OC} = 1.53 V, PCE = 12.578 % (Cs_2TiF_6) and V_{OC} = 8.53 V, PCE = 7.348 % (Cs_2TiCl_6) with the 98 % QE at the visible spectrum of 100-750 nm. This SCAPS device simulation results give us a broader view in selecting the appropriate ETL, HTL to achieve the highest PV performance by reducing the losses.

ACKNOWLEDGEMENTS

The authors are grateful to the Department of Electronics and Information Systems, University of Gent, Belgium and Prof. Burgelman for providing the SCAPS software to carry out this research work. The authors are also thankful to the Science and Engineering Research Board (SERB), Department of Science and Technology (DST) India for their financial support (EMR/2016/002430) to carry out this research work.

REFERENCES

1. A. Kojima, K. Teshima, Y. Shirai, T. Miyasaka, *J. Am. Chem. Soc.* **131** No 17, 6050 (2009).
2. F. Giustino, H.J. Snaith, *ACS Energy Lett.* **1** No 6, 1233 (2016).
3. S.D. Stranks, G.E. Eperon, G. Grancini, C. Menelaou, M.J. Alcocer, T. Leijtens, L.M. Herz, A. Petrozza, H.J. Snaith, *Sci.* **342** No 6156, 341 (2013).
4. W.S. Yang, J.H. Noh, N.J. Jeon, Y.C. Kim, S. Ryu, J. Seo, *Sci.* **348** No 6240, 1234 (2015).
5. W.J. Yin, J.H. Yang, J. Kang, Y. Yan, S.H. Wei, *J. Mat. Chem. A* **3** No 17, 8926 (2015).
6. M.G. Ju, M. Chen, Y. Zhou, H.F. Garces, J. Dai, L. Ma, N.P. Padture, X.C. Zeng, *ACS Energy Lett.* **3** No 2, 297 (2018).
7. M. Chen, M.G. Ju, A.D. Carl, Y. Zong, R.L. Grimm, J. Gu, X.C. Zeng, Y. Zhou, N.P. Padture, *Joule* **23** No 3, 558 (2018).
8. S. Paul, S. Grover, I.L. Repins, B.M. Keyes, M.A. Contreras, K. Ramanathan, R. Noufi, Z. Zhao, F. Liao, J.V. Li, *IEEE J. Photovoltaics* **8** No 3, 023107 (2018).
9. K. Chakraborty, M.G. Choudhury, S. Paul, *Sol. Energy* **194** No 12, 886 (2019).
10. S.K. Pandey, S. Somay, *IEEE Trans. Electron. Dev.* **67** No 10, 4321 (2020).
11. N. Rai, S. Rai, P.K. Singh, P. Lohia, D.K. Dwivedi, *J. Mater. Sci: Mater. Electron.* **31** No 8, 16269 (2020).
12. K. Chakraborty, S. Paul, U. Mukherjee, S.Das, *J. Nano Electron. Phys.* **13** No 3, 03009 (2021).
13. K. Chakraborty, M.G. Choudhury, S. Paul, *IEEE Trans. Device Mater. Reliab.* **21** No 4, 465 (2021).
14. K. Tan, P. Lin, G. Wang, Y. Liu, Z. Xu, Y. Lin, *Solid-State Electron.* **126** No 12, 75 (2016).
15. K. Chakraborty, M.G. Choudhury, S. Paul, *IEEE J. Photovoltaics* **11** No 2, 386 (2021).
16. N. Chaudhary, R. Chaudhary, *J. Mater. Chem. C* **3** No 45, 11886 (2015).
17. Y. Yang, J. You, *Nature* **544** No 4, 155 (2017).
18. A. Zhang, Y. Chen, J. Yan, *IEEE J. Quant. Electron.* **52** No 6, 1600106 (2016).

Чисельний аналіз експлуатаційних характеристик різних матеріалів ETL для перовскітних сонячних елементів на основі одногалогенідного цезію-титану (IV)

Kunal Chakraborty[1], S.V. Kumari[2], Sri Harsha Arigela[3], Mahua Gupta Choudhury[1], Sudipta Das[4], Samrat Paul[1]

[1] *Department of Energy Engineering, North-Eastern Hill University, Shillong, Meghalaya, India*
[2] *Department of ECE, NRI Institute of Technology, Agiripalli, Krishna Dist, AP, India*
[3] *Department of Mechanical Engineering, Koneru Lakshmaiah Education Foundation, Guntur, AP, India*
[4] *Department of ECE, IMPS College of Engineering and Technology, Nityanandapur, Malda, W.B, India*

Безсвинцеві перовскітні сонячні елементи (PSCs) є серйозним конкурентом тонкоплівкової фотоелектричної (PV) технології, оскільки вони вирішують дві основні проблеми: токсичність та стабільність. PSCs на основі Ti є необхідними у високопродуктивних PV пристроях. Зовнішня квантова ефективність (EQE), або класична ефективність, часто використовується для вимірювання оптичних характеристик пристрою на сонячних елементах. Робота спрямована на оптимізацію ETL/HTL та інших інтерфейсів для отримання найбільш ефективного PSC $Cs_2TiI_{6-x}Br_x$, а вдосконалення J_{sc} збільшить рекомбінацію Шоклі-Рід-Холла (SRH). У таких обставинах вибір та оптимізація матеріалів транспортних шарів електронів (ETLs) і дірок (HTLs) є основним фактором, який необхідно ефективно розглядати для досягнення оптимальної PV продуктивності. Серед усіх ETLs, TiO_2 є найбільш підходящим ETL для запропонованих нами *n*-i-*p* структурованих PSCs на основі FTO/ETLs/Cs_2TiX_6/HTL/Ag. Оптимальна товщина ETL повинна бути 150-200 нм, а HTL – 10-20 нм, з наступними оптимізованими PV характеристиками: V_{oc} = 1.23 В, J_{sc} = 19.378 мА/см^2, PCE = 14.537 % (Cs_2TiBr_6); V_{oc} = 1.09 В, J_{sc} = 23.213 мА/см^2, PCE = 17.452 % (Cs_2TiI_6); V_{oc} = 1.53 В, J_{sc} = 16.822 мА/см^2, PCE = 12.578 % (Cs_2TiF_6) and V_{oc} = 8.53 В, J_{sc} = 10.079 мА/см^2, PCE = 7.348 % (Cs_2TiCl_6). Таким чином, детальне вивчення цього класу матеріалів, які містять галогенідний перовскіт, є потребою часу.

Ключові слова: Галогенід, Перовскіт, SCAPS-1D, Фотоелектричний, PCE.